

9-1-2018

Vertical vs. Adiabatic Ionization Energies in Solution and Gas-Phase: Probing Ionization-Induced Reorganization in Conformationally-Mobile Bichromophoric Actuators Using Photoelectron Spectroscopy, Electrochemistry and Theory

Maxim Vadimovich Ivanov
Marquette University

Denan Wang
Marquette University, denan.wang@marquette.edu

Depeng Zhang
Marquette University

Rajendra Rathore
Marquette University, rajendra.rathore@marquette.edu

Scott A. Reid
Marquette University, scott.reid@marquette.edu

Accepted version. *Physical Chemistry Chemical Physics*, Vol. 20, No. 40 (September 2018): 25615-25622. DOI. © 2018 Royal Society of Chemistry. Used with permission.

Marquette University

e-Publications@Marquette

Chemistry Faculty Research and Publications/College of Arts and Sciences

This paper is NOT THE PUBLISHED VERSION; but the author's final, peer-reviewed manuscript. The published version may be accessed by following the link in the citation below.

Physical Chemistry Chemical Physics, Vol. 20, No. 40 (September 2018): 25615-25622. [DOI](#). This article is © Royal Society of Chemistry and permission has been granted for this version to appear in [e-Publications@Marquette](#). Royal Society of Chemistry does not grant permission for this article to be further copied/distributed or hosted elsewhere without the express permission from Royal Society of Chemistry.

Vertical vs. Adiabatic Ionization Energies in Solution and Gas-Phase: Probing Ionization-Induced Reorganization in Conformationally-Mobile Bichromophoric Actuators Using Photoelectron Spectroscopy, Electrochemistry and Theory

Maxim V. Ivanov

Department of Chemistry, Marquette University, Milwaukee, WI

Denan Wang

Department of Chemistry, Marquette University, Milwaukee, WI

Depeng Zhang

Department of Chemistry, Marquette University, Milwaukee, WI

Rajendra Rathore

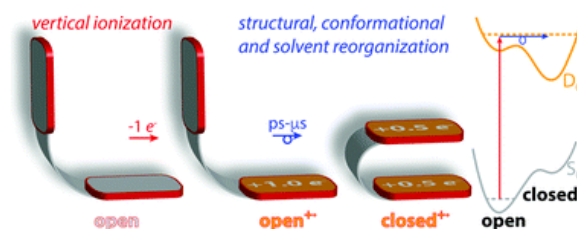
Department of Chemistry, Marquette University, Milwaukee, WI

Scott A. Reid

Department of Chemistry, Marquette University, Milwaukee, WI

Abstract

Ionization-induced structural and conformational reorganization in various π -stacked dimers and covalently linked bichromophores is relevant to many processes in biological systems and functional materials. In this work, we examine the role of structural, conformational, and solvent reorganization in a set of conformationally mobile bichromophoric donors, using a combination of gas-phase photoelectron spectroscopy, solution-phase electrochemistry, and density functional theory (DFT) calculations. Photoelectron spectral analysis yields both adiabatic and vertical ionization energies (AIE/VIE), which are compared with measured (adiabatic) solution-phase oxidation potentials (E_{ox}). Importantly, we find a strong correlation of E_{ox} with AIE, but not VIE, reflecting variations in the attendant structural/conformational reorganization upon ionization. A careful comparison of the experimental data with the DFT calculations allowed us to probe the extent of charge stabilization in the gas phase and solution and to parse the reorganizational energy into its various components. This study highlights the importance of a synergistic approach of experiment and theory to study ionization-induced structural and conformational reorganization.



Introduction

Charge and energy delocalization across π -stacked assemblies is of critical importance in a variety of biological systems and functional materials.¹⁻⁵ Various π -stacked dimers and covalently linked bichromophores undergo appreciable ionization-induced structural (*e.g.*, bond length) changes, as well as conformational reorganization, driven by charge-resonance interactions.⁶⁻⁹ Past studies have established that upon ionization, π -stacked assemblies adopt a cofacial arrangement, where through-space orbital overlap and interchromophoric electronic coupling are maximal. While the enthalpy gain of a complete cofacial approach of two aromatic systems may reach ~ 0.35 V,⁷ the overall free energy gain depends significantly on the linker connecting the two chromophores as well as the surrounding environment (*i.e.*, solvent). In this context, an oxidation-induced molecular actuation,¹⁰⁻¹² *i.e.*, reversible change in structure, conformation and/or physical properties in response to external stimuli,¹³⁻¹⁵ represents an ideal case to probe the extent of cationic charge (*i.e.*, hole) stabilization and structural/conformational reorganization in a set of model bichromophoric electron donors.

As illustrated with a model “clam-like” donor in [Fig. 1](#), following Koopman's theorem and the Franck-Condon principle, initial vertical ionization from the HOMO occurs rapidly on the timescale of nuclear motion, producing a highly vibrationally excited cation radical in the D_0 state, which reorganizes on a timescale of ps- μ s.¹⁰ In solution, the solvent serves as a sink of the initial vibrational excitation, and reorganizes to accommodate the relaxed solute. Fundamentally, we seek to understand the dynamics of

structural, conformational, and solvent reorganization, which accompanies ionization in a set of model bichromophoric electron donors.

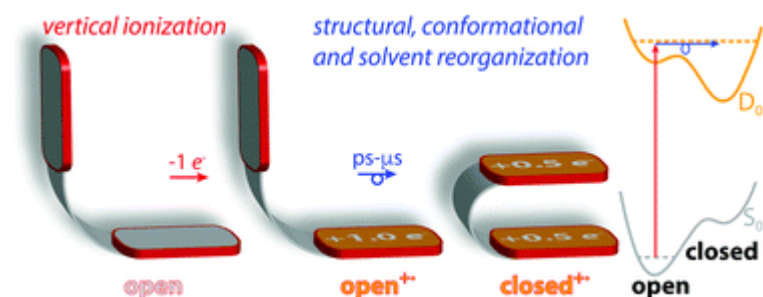


Fig. 1 Illustration of the actuation in a model bichromophoric donor initiated by ionization. The panel at right illustrates the ground (S_0) and ionized (D_0) potential energy surfaces.

The solution phase oxidation potential (E_{ox}) and gas-phase adiabatic ionization energy (AIE) are expected to linearly correlate with the gas-phase vertical ionization energy (VIE) in a set of structurally similar molecules, bearing similar ionization-induced reorganization.^{16–18} A linear correlation with near-unity slope further evidences a similar degree of solvent reorganization.^{16,17} However, in cases of significant structural and/or conformational reorganization, one cannot *a priori* expect a linear relationship between these variables – indeed, it is not obvious how these will correlate.

In this manuscript, we examine a set of bichromophoric actuators and their model compounds using photoelectron spectroscopy, electrochemistry, and DFT calculations, to probe the correlation between adiabatic and vertical IEs measured in the gas-phase and adiabatic E_{ox} in solution. Importantly, we find that the AIEs are linearly correlated with E_{ox} , while the VIEs are not well correlated, as the reorganization energy is species dependent. The variety of donors employed allows us to parse the reorganization energy into its various components, providing deeper insight into the mechanisms of actuation in these prototypical systems.

Results and discussion

Synthesis

A series of similar veratrole- and acetal-based actuator molecules (**V2**, **V2**-locked, **Ac2**-C2H4, **Ac2**-CH2) and model compound **V1** were synthesized from previously reported procedures^{10–12} and were fully characterized by $^1\text{H}/^{13}\text{C}$ NMR spectroscopy. Gas-phase photoelectron spectra of all compounds were recorded at the Center for Gas-Phase Electron Spectroscopy at The University of Arizona.

Adiabatic ionization in solution

A detailed investigation of the ionization-induced actuation of **V2**, **V2**-locked, **Ac2**-C2H4 and **Ac2**-CH2 bichromophores in CH_2Cl_2 solution has been established in previous studies,^{10–12} which showed that **V2** in solution exists in an open conformation and undergoes ionization-induced folding into a closed conformation on a μs timescale (Fig. 2).^{10,11} Electrochemical analysis showed that a cofacial arrangement of veratroles in the closed conformation effectively stabilizes cationic charge (*i.e.*, hole), as evidenced by a significant ($\Delta E_{ox} = -0.26$ V) lowering of its first oxidation potential (E_{ox}) in comparison with the monochromophoric **V1** (Fig. 2). Furthermore, analysis of the X-ray structures of neutral **V2** and its cation

radical salt [**V2**⁺SbCl₆⁻] showed that in addition to the ionization-induced conformational reorganization, structural reorganization occurs in the form of the contraction and elongation of the bond lengths, and this structural reorganization is evenly distributed over both veratrole moieties. Although the relative energetic contributions of structural and conformational reorganizations may not be *a priori* apparent, both contribute toward the observed lowering of the oxidation potential.

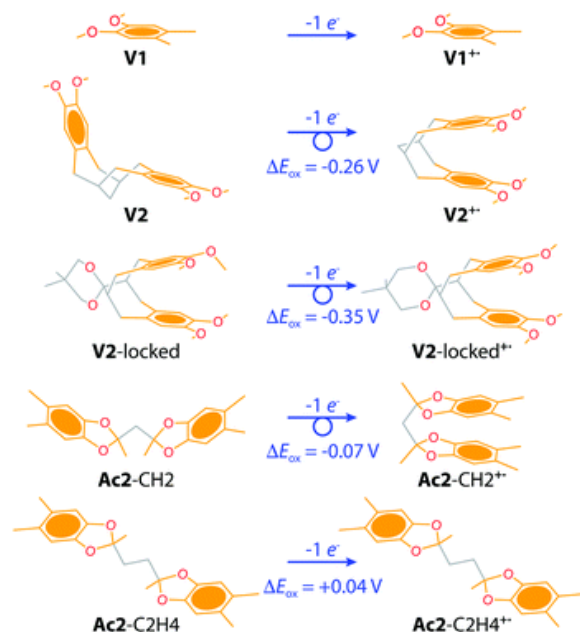


Fig. 2 Illustration of the ionization-induced reorganization in a set of bichromophores and model compound **V1** in CH₂Cl₂ solution.^{10–12} Straight solid line denotes structural reorganization, circle represents additional conformational reorganization, *i.e.*, folding in **V2** and **Ac2-CH2** and methoxy group rotation in **V2-locked**. The $\Delta E_{\text{ox}} = E_{\text{ox}}[\text{bichromophore}] - E_{\text{ox}}[\mathbf{V1}]$ reflects stabilization of the cationic charge.

In contrast, the bichromophore **V2-locked** (Fig. 2) is a rigid structure that exists in a (closed) cofacial arrangement in both neutral and cation radical states. Interestingly, the X-ray structure of neutral **V2-locked** showed that one of the methoxy groups exists in an out-of-plane arrangement (C–O–C_{Ar}–C_{Ar} dihedral angle $\phi = 66.9^\circ$) stabilized by intramolecular hydrogen bond interactions. It is then expected that upon ionization of **V2-locked** in solution, in addition to the structural reorganization in the form of bond length changes, the planarization of the methoxy group will also occur.^{18,19} We note that the methoxy-group orientation in the neutral state of veratrole-containing species is occasionally found out of the aromatic plane. For example, analysis of crystal structures from the CCDC database²⁰ revealed that among 2774 structures containing the veratrole moiety, 44 structures (or 1.6%) have a C–O–C_{Ar}–C_{Ar} dihedral angle in the 54°–110° range (Fig. 3), suggesting that in the neutral state the orientation of the methoxy group is dependent on the local environment and packing. In contrast, available crystal structures of the dimethoxybenzene-based cation radicals showed that methoxy groups exist exclusively in the in-plane arrangement.^{7,10,11,18,19}

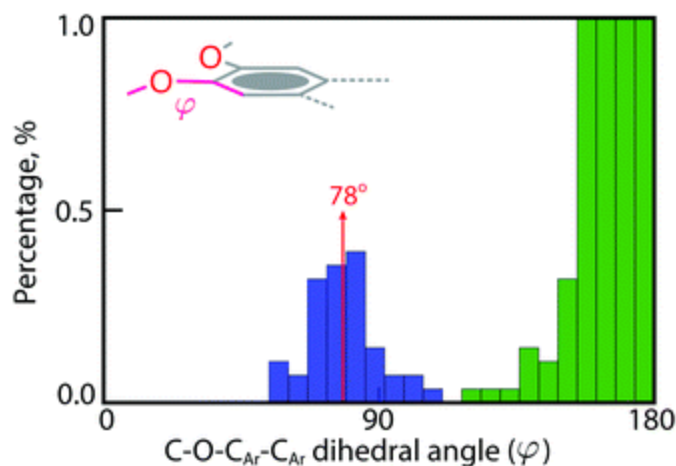


Fig. 3 Distribution of the C–O–C_{Ar}–C_{Ar} dihedral angle obtained from 2774 crystal structures containing veratrole moiety from CCDC database. Note that 90% of the structures have C–O–C_{Ar}–C_{Ar} dihedral angle in 167°–180° range.

Optical spectroscopy and X-ray crystallography of the dimethylcatechol acetals **Ac2-CH2** and **Ac2-C2H4** revealed that both bichromophores exist in the open conformation in the neutral state.¹² Only **Ac2-CH2** undergoes ionization-induced folding into a closed conformation, while **Ac2-C2H4** remains in the open conformation, as evidenced by the lowering of the oxidation potential of **Ac2-CH2** with respect to the model **V1** ($\Delta E_{\text{ox}} = -0.07$ V), and by the absence of any cationic charge stabilization in **Ac2-C2H4** ($\Delta E_{\text{ox}} = 0.04$ V, [Fig. 2](#)). Although the global minimum structures have been identified in solution, they may be different from those existing in the gas phase, especially in the cases when the conformations are nearly isoenergetic and environment-dependent.

Vertical and adiabatic ionization energies in gas phase

Panels A, B and C in [Fig. 4](#) present a schematic of a gas-phase photoelectron experiment, illustrating the difference between vertical and adiabatic ionization energies (VIE and AIE, respectively), a point central to this work. Panel A shows potential curves for a model one-dimensional (*i.e.*, diatomic) case, and transition energies associated with adiabatic and vertical ionization. In a model photoelectron spectrum, panel B, individual vibrational features are distinguished, readily affording AIE and VIE determination. A more realistic case, panel C, shows unresolved features – here, the VIE corresponds to the peak in the photoelectron spectrum, while the AIE can be estimated by linear extrapolation of the rising edge back to the baseline. As such, difference between AIE and VIE measures the extent of combined structural and conformational reorganization upon ionization.

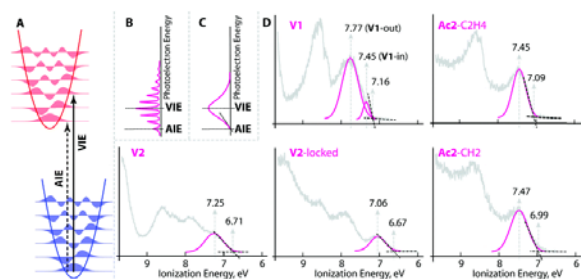


Fig. 4 (A) Schematic one-dimensional harmonic potential energy curves for neutral (blue) and cation radical (red) states with the energy levels corresponding to the vibrational states. The adiabatic and vertical ionization energies are shown (AIE and VIE, respectively). (B) Photoelectron spectra illustrated for a resolved case. Energies corresponding to AIE and

VIE are shown. (C) Illustration of how AIE and VIE are determined for a case where vibrational structure is not resolved. (D) Gas-phase photoelectron spectra of the molecules considered in this work, with derived AIE and VIE values.

Following this procedure, photoelectron spectra of the gas-phase molecules were analyzed and the values of VIE and AIE were obtained (Table 1). In each case the photoelectron spectrum shows a series of broad transitions (Fig. 4D) reflecting electron ejection from various molecular orbitals (MOs), or from different conformations. In particular, analysis of the photoelectron spectrum of **V1** showed that it can be best reproduced if two Gaussian functions are centered at 7.45 and 7.77 eV corresponding to two conformations with the in-plane (**V1-in**) and out-of-plane (**V1-out**) orientation of the methoxy group (Fig. S17 in ESI†) as further supported by the DFT calculations.

Table 1 Experimental adiabatic oxidation potentials (E_{ox}) in CH_2Cl_2 , vertical and adiabatic ionization energies (VIE and AIE, respectively) in the gas phase. VIE and AIE are reproducible to 0.02 and 0.04 eV, respectively

| Compound | E_{ox} , V vs. Fc/Fc^+ | VIE, eV | AIE, eV |
|------------------|--|---------|---------|
| V1 | 0.77 | 7.45 | 7.16 |
| V2 | 0.51 | 7.25 | 6.71 |
| V2-locked | 0.42 | 7.06 | 6.67 |
| Ac2-CH2 | 0.70 | 7.47 | 6.99 |
| Ac2-C2H4 | 0.81 | 7.45 | 7.09 |

The correlation plot between solution-phase E_{ox} and gas-phase AIE shows a clear linear correlation ($R^2 = 0.96$, red circles in Fig. 5), suggesting that the combined structural and conformational reorganization in the gas phase is energetically similar to that in the solution, while a non-unity slope of 0.68 reflects some variance in solvent reorganization. In contrast, the correlation between E_{ox} and VIE shows a scattered plot, which can be separated into a roughly linear trend for compounds that undergo conformational reorganization such as folding and methoxy group rotation (*i.e.*, **V1-out**, **V2**, **V2-locked**, and **Ac2-CH2**, see blue circles in Fig. 5), and a cluster of two molecules where ionization-induced reorganization is limited to the structural reorganization of a single aromatic moiety (*i.e.*, **V1-in**, **Ac2-C2H4**, see blue squares in Fig. 5).

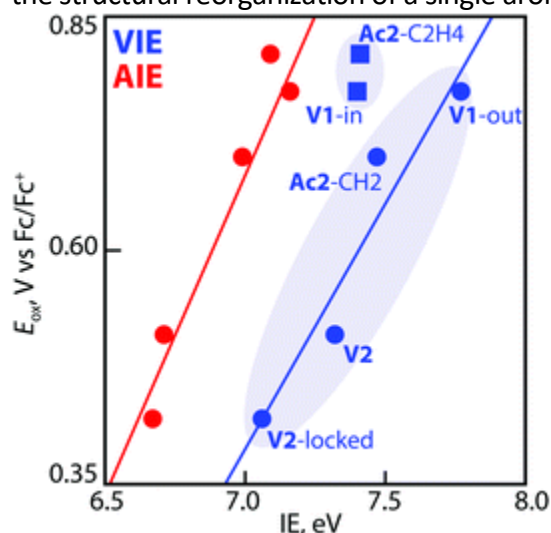


Fig. 5 Correlation plots of the solution phase adiabatic oxidation potentials (E_{ox}) vs. gas-phase adiabatic (red circles) and vertical (blue circles and squares) ionization energies. Best-fit linear trends are shown: $E_{ox} = 0.68\text{AIE} - 4.10$, $R^2 = 0.96$ (red) and $E_{ox} = 0.52\text{VIE} - 3.23$, $R^2 = 0.94$ (blue, **V1-in** and **Ac2-C2H4** excluded).

Overall, the difference in ionization energies ($VIE - AIE = \Delta IE$) reflects the geometrical (structural and conformational) reorganization attendant to ionization, while the value of the slopes in E_{ox} -vs.-AIE and E_{ox} -vs.-VIE dependences reflect solvent reorganization. In order to correctly assess the ionization-induced reorganization, we must identify the global-minimum structures for neutral and cation radical potential energy surfaces in both gas phase and solution. Although the global minimum structures have been experimentally identified in solution, the experimental identification of the global minimum structures in the gas phase is less obvious and, therefore, we resorted to density functional theory calculations.

Computational modelling of the adiabatic and vertical ionizations in the gas phase and solution

Accurate modeling of the ionization-induced actuation in the systems studied in this work presents a challenge for electronic structure calculations, and density functional theory (DFT) in particular, for several reasons.²¹ First, local and gradient-corrected density functionals cannot describe (attractive) long-range dispersion interactions and therefore total energies of the closed conformations of **V2**, **Ac2**-C₂H₄ and **Ac2**-CH₂ are expected to be significantly overestimated using these functionals.²²⁻²⁴ Second, in the ionized state self-interaction error (SIE) may cause an artificial delocalization of the cationic charge leading to underestimated ionization energies of both open and closed conformations.²⁵⁻²⁷ Third, basis set superposition error (BSSE) is expected to be highly conformation-dependent, with the total energies of the closed conformations being underestimated as compared to the open conformations.²⁸ Thus, the method of choice must include dispersion interactions (*e.g.*, via an added empirical term²⁹ or explicit van der Waals functionals³⁰), account for SIE (*e.g.*, using a hybrid functional with fine-tuned amount of the Hartree–Fock exchange³¹ or range-separated functional³²) and include BSSE correction (*e.g.*, using a larger basis set or applying a counterpoise correction^{33,34}).

We have recently shown³⁵ in a combined experimental/theoretical study that CAM-B3LYP³⁶ and B1LYP with 40% of Hartree–Fock exchange (*i.e.*, B1LYP40)³⁷ accurately reproduce experimental binding energies of the van der Waals dimer of fluorene in neutral, excited and cation radical states if the missing dispersion interactions are accounted for using the empirical Grimme's D-3 term, with BSSE correction using the counterpoise (CP) method. In intermolecular complexes the BSSE often arises due to the lack of flexibility of the basis set of each monomer leading to the wrong binding energies or even to incorrect geometries and vibrational frequencies.³⁸⁻⁴⁰ When calculating the binding energy of a dimer using the CP method, the energy of each monomer (or fragment) is calculated using the basis set of both monomers in a dimer. While in the case of intermolecular complexes the definition of a fragment is obvious, in the case of covalently linked bichromophores, a choice of atomic composition, charge and multiplicity of each fragment becomes ambiguous. Despite this arbitrariness, the CP method has been applied in several systems to account for intramolecular BSSE with satisfactory results.⁴⁰⁻⁴²

Here, we have performed electronic structure calculations using CAM-B3LYP-D3 and B1LYP40-D3 functionals and 6-31G(d) basis set with the BSSE correction using the CP method. All actuators were separated into three fragments, *i.e.*, two aromatic moieties and the linker (Fig. 6). To account for the solvents effects we use the polarizable continuum model (PCM) with CH₂Cl₂ as a solvent. See ESI† for full computational details.

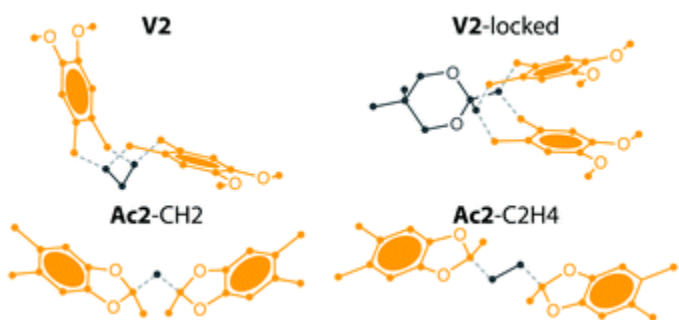


Fig. 6 Fragments of the actuators used in the CP method. See Fig. S18 in ESI[†] for alternative approach.

We first confirmed that calculations can accurately identify the global minimum structures of the actuators in solution. Indeed, in agreement with the experimental data, CAM-B3LYP-D3/6-31G(d) + PCM(CH₂Cl₂) calculations predict that actuators **V2**, **Ac2-C2H4** and **Ac2-CH2** in the neutral state prefer an open conformation, albeit with varied difference in free energies. For **V2** and **Ac2-C2H4**, the open conformer is 2.1 and 3.5 kcal mol⁻¹ lower in energy than closed, respectively, while in the case of **Ac2-CH2** the two conformers are isoenergetic. As the orientation of the methoxy group in the neutral state is somewhat uncertain (Fig. 3), we have also considered several conformations of **V1**, **V2** and **V2-locked** with out-of-plane methoxy group orientations (Fig. 7). In agreement with the X-ray crystallography data, calculations show that **V2-locked** with the methoxy group oriented out-of-plane is the most stable, while **V1** and **V2** prefer an in-plane arrangement (blue dashed squares in Fig. 7A). See Tables S1–S16 in ESI[†] for full details.

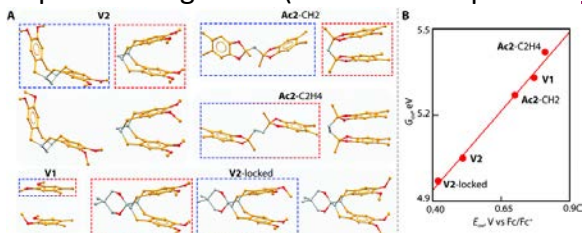


Fig. 7 (A) Equilibrium structures optimized using CAM-B3LYP-D3/6-31G(d) + PCM(CH₂Cl₂). Blue boxes correspond to the global minimum structures of the neutral, red boxes correspond to the global minimum structures of the cation radical. See Tables S1–S16 in ESI[†] for full details. (B) Correlation plot between calculated adiabatic ionization free energies (G_{ox}) and experimental oxidation potentials. Best-fit linear trends is shown: $G_{\text{ox}} = 1.10 E_{\text{ox}} + 4.50$, $R^2 = 0.99$.

For the cation radical state, calculations show that in all cases, except **Ac2-C2H4**, a closed conformation with in-plane arrangement of the methoxy groups is the global minimum energy structure (red dashed squares in Fig. 7A), in complete agreement with experiment (Fig. 2). The energetic difference of the global minimum structures of the cation radical (D_0) and neutral (S_0) states provides the calculated adiabatic ionization free energy (*i.e.*, $G_{\text{ox}} = G[D_0] - G[S_0]$), which upon correlation with experimental oxidation potentials shows a perfect linear trend (Fig. 7B).

In the gas phase, this picture changes significantly, as the various conformations become nearly isoenergetic, with energy differences within 1 kcal mol⁻¹ or less. For example, the gas-phase energy difference of **V2** in open and closed conformations with out-of-plane methoxy groups is only 0.75 kcal mol⁻¹ (Table S1 in ESI[†]), while open and closed conformations of **Ac2-CH2** and **Ac2-C2H4** differ by 0.3 and 1.1 kcal mol⁻¹, respectively (Tables S9 and S13 in ESI[†]). In contrast, the calculated vertical ionization energies ($\text{VIE} = E[D_0] - E[S_0]$, at the equilibrium geometry of neutral state) of various conformations depend dramatically on the conformation (*e.g.*, Table S1 in ESI[†]). Indeed, it has been established both experimentally and theoretically that the extent of cofaciality between aromatic moieties and the orientation of the methoxy relative to the aromatic plane are reflected in the values of VIE and E_{ox} .^{18,43} The

high sensitivity of the conformation to the VIE allowed us to pinpoint the conformations that most likely exist in the gas phase by correlating calculated VIEs against experimental values (Fig. 8A). Remarkably, conformations that show the best correlation with experiment correspond exactly to those identified as global minimum structures in solution.

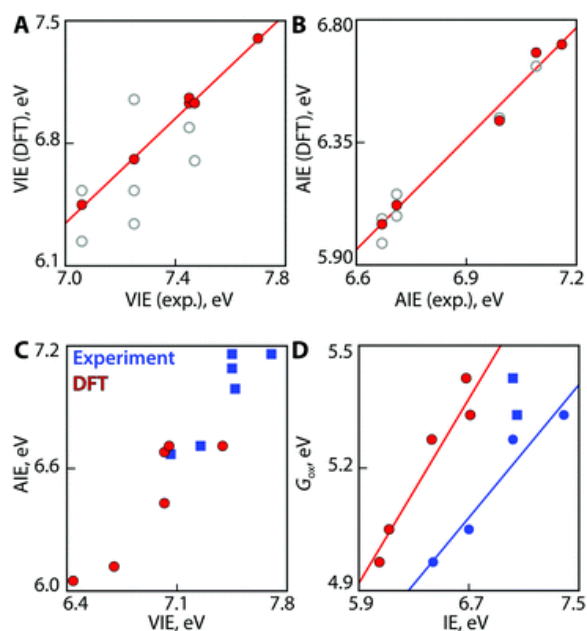


Fig. 8 (A) Correlation plot between VIEs from DFT and experiment. Solid line is the best-fit linear trend $y = 1.50x - 4.13$, $R^2 = 1.00$. In panels A and B, filled red circles correspond to conformations that match best with experimental values, empty grey circles correspond to the remaining conformations. (B) Correlation plot between AIEs from DFT and experiment. Solid line is the best-fit linear trend $y = 1.36x - 3.01$, $R^2 = 0.99$. (C) Correlation plot between AIEs and VIEs obtained from DFT (red circles) and experiment (blue squares). (D) Correlation plots of the calculated solution-phase adiabatic ionization free energies (G_{ox}) against calculated gas-phase adiabatic (red circles) and vertical (blue circles and squares) ionization energies. Best-fit linear trends are shown: $G_{ox} = 0.56AIE + 1.59$, $R^2 = 0.93$ (red) and $G_{ox} = 0.41VIE + 2.35$, $R^2 = 0.94$ (blue, **V1**-in and **Ac2**-C2H4 excluded).

For the cation radical state, our calculations show that the closed conformer bearing an in-plane arrangement of methoxy groups is the global minimum for all molecules, with other conformations being far less stable. Interestingly, in contrast to the solution phase, **Ac2**-C2H4 likely does undergo oxidation-induced folding in gas phase, as the calculated energy of the closed conformation is 3.7 kcal mol⁻¹ lower than that of the open conformer (Table S16 in ESI[†]). The difference between energies of cation radical (D_0) and neutral (S_0) states for the identified equilibrium structures gives adiabatic ionization energies (*i.e.*, $AIE = E[D_0] - E[S_0]$, at the equilibrium geometries of each respective state), that upon correlation with experimental AIEs showed a perfect linear trend (Fig. 8B). Finally, correlations of the calculated VIE with AIE (Fig. 8C, red) and with G_{ox} (Fig. 8D) show a close resemblance to the analogous experimental plots (Fig. 8C, blue and Fig. 5), confirming that our assignment of the oxidation-induced conformational reorganization is consistent with experimental data. Note that although the scatter of the experimental and calculated points in Fig. 8C is nearly identical, the calculated values are underestimated by a constant offset value of 0.6 eV.

Probing the extent of hole stabilization and ionization-induced reorganization in the gas phase

A detailed analysis of the experimental vertical and adiabatic ionization energies in gas phase and solution, with the aid of extensive calculations, allowed us to pinpoint conformational reorganization attendant to vertical ionization in the gas phase and solution. While the ionization-induced actuation in the gas phase involves (overall) similar conformational reorganization as in solution, there are a few distinct features. For example, the degree of cationic charge (*i.e.*, hole) stabilization is much more prominent in the gas phase than in solution, as evidenced by a significant lowering of the AIE, as compared to **V1**, *e.g.*, $\Delta\text{AIE}[\mathbf{V2}] = -0.45$ eV and $\Delta\text{AIE}[\mathbf{V2}\text{-locked}] = -0.49$ eV (Fig. 9). Analogous quantities in solution are significantly more modest, *i.e.*, $\Delta E_{\text{ox}}[\mathbf{V2}] = -0.26$ V and $\Delta E_{\text{ox}}[\mathbf{V2}\text{-locked}] = -0.35$ V, with the difference arising due to additional solvent reorganization. Furthermore, the degree of hole stabilization is highly dependent on the linker and spans a significant range, *i.e.*, -0.49 to -0.07 eV (Fig. 9). Finally, the nearly nonexistent hole stabilization of -0.07 eV in **Ac2-C2H4** in the gas-phase is reflected in the absence of oxidation-induced folding in the solution phase due to the additional solvent reorganization (compare, *e.g.*, Fig. 2 and 9).

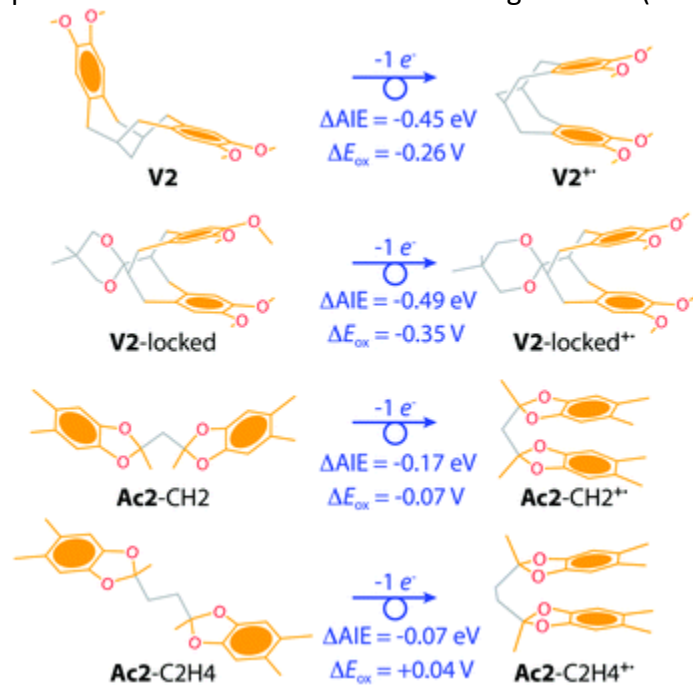


Fig. 9 Illustration of the ionization-induced reorganization in a set of bichromophores in the gas phase. The $\Delta\text{AIE} = \text{AIE}[\text{actuator}] - \text{AIE}[\mathbf{V1}]$ reflects stabilization of the cationic charge in gas phase.

Although the relative energetic contributions of structural and conformational reorganizations are not *a priori* apparent, a close inspection of the difference in ionization energies ($\text{VIE} - \text{AIE} = \Delta\text{IE}$) allows us to separate these components. Considering the monomeric models **V1-in** and **V1-out** (Table S17 in ESI[†]), the former undergoes only structural reorganization with attendant bond length changes ($\Delta\text{IE} = \text{VIE} - \text{AIE} = 0.29$ eV), while the latter also exhibits conformational reorganization, as the methoxy group rotates into the molecular plane upon ionization ($\Delta\text{IE} = 0.54$ eV). Both of these components are present also in the rigid **V2-locked**, which has a somewhat similar ΔIE of 0.39 eV. In contrast, the foldable **V2** shows a larger ΔIE of 0.54 eV, reflecting the additional conformational reorganization associated with folding (Fig. 9). Moving to the acetal-based actuators, **Ac2-CH2** and **Ac2-C2H4** exhibit relatively (*e.g.*, to **V2**) smaller reorganization energy of 0.48 and 0.36 eV, respectively, despite the presence of both structural and conformational (*i.e.*, folding)

reorganization. This analysis highlights the importance of the alkyl framework linking two chromophores in controlling the extent of structural and conformational reorganization.

Considering the role of solvent, previously Parker¹⁶ and Kochi and co-workers¹⁷ have shown a strong linear correlation of oxidation potentials and VIE in a set of structurally similar molecules. In the former case, a near unity slope was derived, while the latter case found a slope less than unity (~ 0.71), which was suggested to reflect differences in the energy of solvation. Our derived slope for the correlation of E_{ox} and AIE (Fig. 5) is of a somewhat similar magnitude (0.52), suggesting some (linear) variations in solvent reorganization amongst this set of actuators.

Role of intramolecular basis set superposition error (BSSE)

While it is widely accepted that the BSSE is critically important for accurate prediction of the binding energies in the intermolecular complexes, the importance of intramolecular BSSE is less recognized. Here, the availability of a set of conformationally-mobile bichromophores with access to π -stacked (*i.e.*, closed) conformations present a unique opportunity to probe the role of intramolecular BSSE; and complete data is summarized in Tables S18 and S19 in ESI.[†]

First, we expect that the BSSE should be larger for the closed conformations as compared to open. Indeed, depending on the bichromophore the difference in BSSE, *i.e.*, $\Delta BSSE = BSSE[\text{closed}] - BSSE[\text{open}]$, varies from 2.8 kcal mol⁻¹ in **V2** to 1.1 kcal mol⁻¹ in **Ac2-CH2** to 0.6 kcal mol⁻¹ in **Ac2-C2H4**. These relatively minor differences are, however, sufficient to incorrectly assign global minimum conformations of **V2** and **Ac2-CH2** if the BSSE is not corrected. At the same time, the varied orientation of the methoxy groups adds an additional 0.0–0.4 kcal mol⁻¹ to the BSSE. Interestingly, for the cation radical state the BSSE is generally smaller, by 0.6–2.4 kcal mol⁻¹, than in the neutral state. Yet, the BSSE of the cation radical state is also conformation-dependent and is the largest for closed conformations. Due to a significant overall stabilization of the closed conformation at the cation radical, absence of BSSE correction does not lead to errors in assignment of the global minimum structures.

Finally, the choice of the atomic composition, spin and multiplicity of the fragments in the counterpoise (CP) method implies uncertainty in the estimate of BSSE correction. For example, when the molecule is fragmented differently than that shown in Fig. 6 (see Fig. S18 in ESI[†]), the BSSE differs by less than 2.1 kcal mol⁻¹ in **V2** and **V2-locked** and by 3.8–6.0 kcal mol⁻¹ in **Ac2-CH2** and **Ac2-C2H4**. Such a significant difference for **Ac2-CH2** and **Ac2-C2H4** arises from the completely different electronic structures of the isolated fragments in the two approaches (Fig. S18 in ESI[†]). We thus conclude that the counterpoise correction is more reliable when the electronic structure of the isolated fragment is close to the electronic structure of that fragment within the molecule.⁴¹ Importantly, we recognize that the only method to fully eliminate BSSE is to increase the size of the basis set, which may not be practical.²⁸

Conclusions

In this work, we have examined structural, conformational, and solvent reorganization in a set of conformationally mobile bichromophoric donors (*i.e.*, actuators), *via* gas-phase photoelectron spectroscopy, solution phase electrochemistry, and DFT calculations. From gas-phase photoelectron spectra, both adiabatic and vertical ionization energies (AIE/VIE) were derived, which we compared with measured solution phase oxidation potentials (E_{ox}). A strong correlation was found of E_{ox} with AIE, but not VIE, reflecting variations in structural and/or conformational reorganization upon ionization. These changes were further delineated *via* a detailed conformational analysis, using a combination of DFT calculations and experimental data. This analysis allowed us to pinpoint the extent of hole stabilization in various actuators

and parse the reorganization energy into its various components, providing deeper insight into the mechanisms of actuation in these model compounds. Finally, we noted the importance of the intramolecular basis set superposition error in accurately predicting potential energy surfaces when π -stacked (*i.e.*, closed) conformations are present. Overall, this study highlights the importance of a synergistic approach of experiment and theory in the study of ionization-induced conformational and structural reorganization.

Conflicts of interest

There are no conflicts to declare.

Acknowledgements

We thank the NSF (CHE-1508677) and NIH (R01-HL112639-04) for financial support, Dr Nadine E. Gruhn for photoelectron spectroscopy and Prof. Qadir Timerghazin for helpful discussions. The calculations were performed on the high-performance computing cluster Père at Marquette University and the Extreme Science and Engineering Discovery Environment (XSEDE).

Notes and references

1. Z. Zheng, N. R. Tummala, Y.-T. Fu, V. Coropceanu and J.-L. Brédas, *ACS Appl. Mater. Interfaces*, 2017, **9**, 18095 - 18102
2. D. B. Bucher, B. M. Pilles, T. Carell and W. Zinth, *Proc. Natl. Acad. Sci. U. S. A.*, 2014, **111**, 4369 -4374
3. T. M. Wilson, T. A. Zeidan, M. Hariharan, F. D. Lewis and M. R. Wasielewski, *Angew. Chem., Int. Ed. Engl.*, 2010, **49**, 2385 -2388
4. J. Casado, K. Takimiya, T. Otsubo, F. J. Ramírez, J. J. Quirante, R. Ponce Ortiz, S. R. González, M. Moreno Oliva and J. T. López Navarrete, *J. Am. Chem. Soc.*, 2008, **130**, 14028 -14029
5. G. C. Solomon, C. Herrmann, J. Vura-Weis, M. R. Wasielewski and M. A. Ratner, *J. Am. Chem. Soc.*, 2010, **132**, 7887 -7889
6. M. V. Ivanov, N. J. Reilly, B. Uhler, D. Kokkin, R. Rathore and S. A. Reid, *J. Phys. Chem. Lett.*, 2017, **8**, 5272 -5276
7. T. S. Navale, K. Thakur, V. S. Vyas, S. H. Wadumethrige, R. Shukla, S. V. Lindeman and R. Rathore, *Langmuir*, 2012, **28**, 71 -83
8. A. A. Zadorozhnaya and A. I. Krylov, *J. Chem. Theory Comput.*, 2010, **6**, 705 -717
9. K. B. Bravaya, O. Kostko, M. Ahmed and A. I. Krylov, *Phys. Chem. Chem. Phys.*, 2010, **12**, 2292 -2307
10. R. Shukla, K. Thakur, V. J. Chebny, S. A. Reid and R. Rathore, *J. Phys. Chem. B*, 2010, **114**, 14592 -14595
11. V. J. Chebny, R. Shukla, S. V. Lindeman and R. Rathore, *Org. Lett.*, 2009, **11**, 1939 -1942
12. R. Rathore, V. J. Chebny, E. J. Kopatz and I. A. Guzei, *Angew. Chem., Int. Ed.*, 2005, **44**, 2771 -2774
13. Y. Wang, J. Sun, Z. Liu, M. S. Nassar, Y. Y. Botros and J. F. Stoddart, *Chem. Sci.*, 2017, **8**, 2562 -2568
14. T. Fukino, H. Yamagishi and T. Aida, *Adv. Mater.*, 2017, **29**
15. P. Beaujean and M. Kertesz, *Theor. Chem. Acc.*, 2015, **134**, 147
16. V. D. Parker *J. Am. Chem. Soc.*, 1976, **98**, 98 -103
17. J. O. Howell, J. M. Goncalves, C. Amatore, L. Klasinc, R. M. Wightman and J. K. Kochi, *J. Am. Chem. Soc.*, 1984, **106**, 3968 -3976
18. M. R. Talipov, A. Boddada, S. V. Lindeman and R. Rathore, *J. Phys. Chem. Lett.*, 2015, **6**, 3373 -3378
19. M. V. Ivanov, D. Wang, S. H. Wadumethridge and R. Rathore, *J. Phys. Chem. Lett.*, 2017, **8**, 4226 -4230
20. C. R. Groom, I. J. Bruno, M. P. Lightfoot and S. C. Ward, *Acta Crystallogr., Sect. B: Struct. Sci., Cryst. Eng. Mater.*, 2016, **72**, 171 -179
21. A. J. Cohen, P. Mori-Sánchez and W. Yang, *Chem. Rev.*, 2012, **112**, 289 -320
22. S. Kristyán and P. Pulay, *Chem. Phys. Lett.*, 1994, **229**, 175 -180

23. S. Ehrlich , J. Moellmann and S. Grimme , *Acc. Chem. Res.*, 2012, **46** , 916 -926
24. P. Kraus , D. A. Obenchain and I. Frank , *J. Phys. Chem. A*, 2018, **122** , 1077 -1087
25. J. L. Bao , L. Gagliardi and D. G. Truhlar , *J. Phys. Chem. Lett.*, 2018, **9** , 2353 -2358
26. M. Lundberg and P. E. M. Siegbahn , *J. Chem. Phys.*, 2005, **122** , 224103
27. Y. Zhang and W. Yang , *J. Chem. Phys.*, 1998, **109** , 2604 -2608
28. F. Jensen *Chem. Phys. Lett.*, 1996, **261** , 633 -636
29. S. Grimme , J. Antony , S. Ehrlich and H. Krieg , *J. Chem. Phys.*, 2010, **132** , 154104
30. K. Berland , V. R. Cooper , K. Lee , E. Schröder , T. Thonhauser , P. Hyldgaard and B. I. Lundqvist , *Rep. Prog. Phys.*, 2015, **78** , 066501
31. M. Renz , K. Theilacker , C. Lambert and M. Kaupp , *J. Am. Chem. Soc.*, 2009, **131** , 16292 -16302
32. R. Baer , E. Livshits and U. Salzner , *Annu. Rev. Phys. Chem.*, 2010, **61** , 85 -109
33. R. Cammi and J. Tomasi , *Theor. Chim. Acta*, 1986, **69** , 11 -22
34. R. Cammi , R. Bonaccorsi and J. Tomasi , *Theor. Chim. Acta*, 1985, **68** , 271 -283
35. D. Kokkin , M. V. Ivanov , J. Loman , J.-Z. Cai , R. Rathore and S. A. Reid , *J. Phys. Chem. Lett.*, 2018, **9** , 2058 -2061
36. T. Yanai , D. P. Tew and N. C. Handy , *Chem. Phys. Lett.*, 2004, **393** , 51 -57
37. M. R. Talipov , A. Boddeda , Q. K. Timerghazin and R. Rathore , *J. Phys. Chem. C*, 2014, **118** , 21400 -21408
38. D. Moran , A. C. Simmonett , F. E. Leach , W. D. Allen , P. V. R. Schleyer and H. F. Schaefer , *J. Am. Chem. Soc.*, 2006, **128** , 9342 -9343
39. J. M. Martin , P. R. Taylor and T. J. Lee , *Chem. Phys. Lett.*, 1997, **275** , 414 -422
40. D. Asturiol , M. Duran and P. Salvador , *J. Chem. Phys.*, 2008, **128** , 144108
41. D. Asturiol , M. Duran and P. Salvador , *J. Chem. Theory Comput.*, 2009, **5** , 2574 -2581
42. R. M. Balabin *J. Chem. Phys.*, 2010, **132** , 211103
43. M. V. Ivanov , S. H. Wadumethrige , D. Wang and R. Rathore , *J. Phys. Chem. C*, 2017, **121** , 15639 -15643